ELSEVIER

Biophysical Chemistry 101–102 (2002) 425–445

Biophysical Chemistry

www.elsevier.com/locate/bpc

Extensions of counterion condensation theory. I. Alternative geometries and finite salt concentration

J. Michael Schurr*, Bryant S. Fujimoto

Department of Chemistry, University of Washington, P.O. Box 351700, Seattle, WA 98195-1700, USA

Received 19 December 2001; accepted 26 February 2002

Abstract

The counterion condensation theory originally proposed by Manning is extended to take account of both finite counterion concentration (m_C) and the actual structure of the array of discrete changes. Counterion condensation is treated here as a binding isotherm problem, in which the unknown free volume is replaced by an unknown local binding constant β', which is expected to vary with m_C and polyion structure. The relation between the condensed fraction of counterion charge, r, β' and m_C is obtained from the relevant grand partition function via the maximum term method. In the case of the single polyion in a large salt reservoir, the result is practically identical to Manning's equation. In order to determine the values of β' and r at arbitrary m_C, a second relation between r, β' and m_C is required. We propose an alternative auxiliary relation that is equivalent to previous assumptions near $m_C=0$, but which yields qualitatively correct and quantitatively useful results at finite m_C. Simple expressions for r vs. m_C and β' vs. m_C are obtained by simultaneously solving the binding isotherm and auxiliary equations. Then r and β' are evaluated for five different linear arrays of infinite extent with different geometries: (1) a straight line of charges with uniform axial spacing; (2) two parallel lines of in-phase uniformly spaced charges; (3) a single-helix of discrete charges with uniform axial spacing; (4) a double-helix of discrete charges with uniform axial spacing of pairs of charges; (5) a cylindrical array of many parallel charged lines, chosen to simulate a uniformly charged cylinder. In all cases, the computed binding isotherms exhibit qualitatively correct behavior. As m_C approaches zero, r approaches the Manning limit, $r=1-1/(L_B/b)$ where b is the average axial spacing of electronic charges in the array and L_B is the Bjerrum length. However, β' varies with polyion geometry, even in the zero salt limit, and matches the Manning value only in the case of a single straight charged line. With increasing m_C, r declines significantly below its limiting value whenever $\lambda b \gtrsim 0.3$, where λ is the Debye screening parameter. In the case of cylindrical arrays containing either 2 or 100 parallel charged lines, r also decreases, whenever $\lambda d \gtrsim 2.0$, where d is the diameter of the array. In the case of two parallel charged lines, each with axial charge spacing $b=3.4$ Å, which are separated by $d=200$ Å, r exhibits a plateau value, 0.76, characteristic of the two combined lines, when $\lambda d \ll 2.0$, and declines with increasing m_C to a shelf value, 0.52, characteristic of either single line, when $\lambda d \gtrsim 2.0$ and the lines become effectively screened from one another. β' behaves in a roughly similar fashion. In the case of a cylindrical array of charged lines with the diameter and linear charge density of DNA, the r-values predicted by the present theory agree fairly well with those predicted by non-linear Poisson–Boltzmann theory up to 0.15 M uni-univalent salt.

Keywords: DNA; Counterion condensation theory; Geometry

*Corresponding author. Tel.: +1-206-543-6681.
E-mail address: schurr@chem.washington.edu (J.M. Schurr).

0301-4622/02/$ - see front matter © 2002 Elsevier Science B.V. All rights reserved.
PII: S0301-4622(02)00178-3

1. Introduction

An important quantity in polyelectrolyte theory is the effective charge that enables the linearized Poisson–Boltzmann (or Debye–Hückel) theory to correctly predict the electrostatic potential in the linear region at large distances from the polyion, and which is important for estimating numerous properties of dilute polyion solutions [1–3]. In principle, this effective charge can be determined by solving the non-linear Poisson–Boltzmann equation or via Monte Carlo simulations, but computational difficulties have so far limited such efforts to either very smooth and regular charge distributions or rather small arrays of discrete charges. The main idea of counterion condensation theory is to avoid such computational difficulties by incorporating a quasi-chemical counterion binding equilibrium in a self-consistent manner directly into the linear theory, where the linear superposition of potentials enormously simplifies the calculations. The counterion condensation theory originally proposed by Manning for infinitely long, straight, linear polyions yields numerous predictions that are in remarkably good agreement with experiments on various polyelectrolytes, including DNA [4–7]. This is especially true in regard to those properties that directly reflect changes in the condensed or bound fraction of counterion charge, such as the release of a fraction of the condensed counterions when DNA melts, the variation of DNA melting temperature with salt concentration, the effect of salt concentration on electrostatic binding equilibria, and variations in polyion electrophoretic mobility with dielectric constant [8,9] and counterion charge [10–12]. Certain other properties that more indirectly reflect the condensed fraction, such as the electrostatic contribution to the persistence length, also agree well with the predictions of counterion condensation theory [13]. Although counterion condensation theory gives a poor account of the electrostatic potential and ion distributions near the polyion surface by comparison with results of non-linear Poisson–Boltzmann theory, [6,14–19] it compares favorably in other regards [20] and is still widely used to estimate the condensed fraction of counterions for polyions in various circumstances, especially those where non-linear Poisson–Boltzmann theory is difficult to apply, for example in bundles containing two or more long linear discretely charged polyions [21–25].

In its original form, counterion condensation theory provided no satisfactory prescription for treating the effects of varying either the counterion concentration m_C or the local polyion geometry on the condensed fraction (r) of counterion charge, while holding the axial spacing (b) of polyion charges constant. Yet it is clear that certain variations in m_C (e.g. increasing, m_C into the region $\lambda b > 1.0$, where λ is the Debye screening parameter) or in polyion structure (e.g. placing the same number of charges per unit axial distance on two widely separated parallel lines rather than on a single line) must strongly affect r for some $m_C > 0$. The effects of finite m_C and polyion structure are both important in studies of polyion bundling. For example, inside a small bundle of parallel polyions, all polyions within a couple of screening lengths of any given polyion interact significantly with that one, and contribute to increase its condensed fraction above the r-value appropriate for a single isolated polyion [22]. Moreover, at finite m_C (or salt concentration) r is expected to become independent of the total number of parallel polyions in the bundle, when the bundle diameter greatly exceeds λ^{-1}.

Previous treatments of the effects of finite counterion concentration [7,9,21,22,26–30] have all implicitly or explicitly assumed that the free volume, or partition function, of a condensed ion is independent of counterion concentration. It seems most unlikely that this assumption is correct for two reasons. (1) From one perspective, the condensed counterion charge merely represents the difference between the actual polyion charge and the effective polyion charge that in the linear Debye–Hückel theory yields the same electrostatic potential as the actual non-linear Poisson–Boltzmann potential in the linear region of the latter, which occurs at large distances from the polyion. In this view, the volume occupied by the condensed fraction of counterions lies inside the linear region, the inner boundary of which moves inward with increasing counterion concentration. Thus, the volume occupied by the condensed counterions is

expected to decrease with increasing salt concentration, as shown by several authors [17,31,32]. (2) From another perspective, the free volume, or partition function of a condensed ion, is not actually the volume occupied by the counterions but instead is an effective binding constant (β') for the association of a counterion with a charged site along the polyion [9]. The interaction of a bound counterion with the neighboring polyion sites is taken into account in the electrostatic free energy of the polyion. However, the electrostatic interaction of each counterion with the particular polyion charge to which it is most proximally bound is not included in that polyion free energy, but is manifested instead as an unknown contribution to the effective site binding constant β' [9]. Because the latter interaction is strongly screened by any salt present, the effective site binding constant, or equivalently the free volume, is expected to decrease with increasing salt concentration.

Nearly all previous treatments of the effects of polyion structure, including finite chain length, on counterion condensation at finite m_C have implicitly assumed that the free volume, or equivalently the effective site binding constant β', is independent of the polyion structure [7,9,21–29]. In explicit evaluations [7,9,26,27] the free volume was usually taken to be the value applicable to an infinite discretely charged line with the same axial charge spacing in the $m_C \rightarrow 0$ limit. It will be demonstrated rigorously below that the free volume, or β', actually depends strongly on polyion structure, even in the $m_C \rightarrow 0$ limit. This point was recently noted by Manning for the case of a single-helix [30]. Consequently, one may not generally employ the free volume applicable to a charged line in the $m_C \rightarrow 0$ limit in order to calculate the condensed fraction r for polyions with alternative structures at finite m_C. In the $m_C \rightarrow 0$ limit, the condensed fraction of counterions is independent of polyion structure and depends only upon the average axial charge spacing b, but the free volume, or β', nevertheless varies with polyion structure, as will be explicitly demonstrated for several alternative structures. For this reason, previous calculations of r for alternative structures that differ from uniform discretely charged lines are almost certainly incorrect, whenever m_C is so large as to cause a significant decrease of r below the limiting value at $m_C = 0$. This point will also be explicitly demonstrated below.

Many earlier treatments of the effects of polyion structure, including finite polyion length, have implicitly or explicitly assumed that both the condensed fraction and free volume were uniform at all sites of the polyion, even when those were energetically and structurally inequivalent [21–27]. As demonstrated by Record et al. [33–38], this assumption is clearly invalid near the ends of charged arrays, although it may be a useful approximation in certain cases, including very long polyions.

Surprisingly, even for very long polyions with uniform axial charge spacing, the presumption that the condensed counterions are distributed uniformly along the polyion is actually contradicted, when the standard mean-field, or mean-occupation, approximation is used to evaluate conventional counterion condensation theory. That approximation actually yields an oscillatory charge distribution, as will be shown in detail in a subsequent communication. Nevertheless, Monte Carlo simulations of the actual distribution of condensed counterions on the lattice (within the conventional counterion condensation theory) exhibit no (or nearly no) oscillations in the distribution of condensed counterions, which demonstrates that such oscillations are artifactual, arising from an essential flaw in the mean-field approximation. This problem and others pertaining to site-to-site variations of the condensed fraction of counterion charge r_j will be addressed in a subsequent paper. In the present treatment of infinite linear arrays of periodically positioned charges, we continue to impose a uniform (non-oscillatory) distribution of polyion charge by assumption at the outset.

If counterion condensation depends upon local polyion structure, it necessarily also depends on the location and orientation of neighboring polyions, and is therefore expected to vary with polyion concentration. This effect was treated using a field theoretic method that is valid in, and only in, the semi-dilute regime [28]. However, that theory, also invokes the assumption of a constant β' that is independent of m_C, of polyion structure, and of the average arrangement of neighboring

polyions, and further assumes that all polyion charges are equivalent in the sense that r and β' are identical for all of them.

1.1. The problem of determining two unknowns from a single equation

A major problem with the original counterion condensation theory for an infinite discretely charged line is that it yields a single binding expression (Eq. (4) below) containing two unknown variables, namely the condensed fraction r and the effective site binding constant β', or free volume. This equation was traditionally solved for both r and β' in the limit $m_C \to 0$ by invoking an auxiliary assumption, namely that β' is constant, or $d\beta'/dm_C = 0$. Provided that $d\beta'/dm_C$ is not infinite, the binding expression exhibits singular behavior in the limit $m_C \to 0$, namely an infinite discontinuity of its right-hand side (rhs) as a function of r. Consequently, it yields a unique value for r, which is robust in the sense that it 'solves' the binding expression regardless of the value of β', and is itself independent of β', in the $m_C \to 0$ limit. That is, for any given constant value of β', the corresponding value of r that solves the binding expression can be brought arbitrarily close to the unique limiting value simply by decreasing m_C to a sufficiently small value. The clear implication of such singular behavior is that β' cannot actually be determined from the binding expression in the limit $m_C = 0$ without invoking a second auxiliary assumption. In the traditional approach [4,5], it is implicitly assumed that $dr/dm_C \cong 0$, as well as $d\beta'/dm_C = 0$, in the domain of small m_C, and the binding expression is then solved for β' at some implicitly very small, but non-vanishing, value of m_C, such that r retains its limiting value, but the rhs of the binding expression no longer exhibits a discontinuity as a function of r, so a unique value of β' can be determined. A third assumption that β' is independent of polyion geometry in the $m_C \to 0$ limit is demonstrably incorrect under the assumptions of the traditional approach just described, and is unnecessary for any array wherein the interaction sum can be evaluated in the $m_C \to 0$ limit. For the latter reason, this third assumption is not counted among the two auxiliary assumptions of the traditional approach.

1.2. Principal objectives

Our objectives here are as follows: (1) We shall review the assumptions invoked in previous treatments of counterion condensation at finite m_C. The qualitatively incorrect predictions stemming from the (incorrect) assumption that β' is a constant independent of m_C will be explicitly demonstrated. (2) We shall extend counterion condensation theory for infinite linearly extended arrays of equivalent charges in such a way that both β' (or the free volume) and r are allowed to vary with m_C and with array geometry. This is accomplished by invoking a less restrictive assumption than those employed in the previous treatments discussed above. This new auxiliary assumption yields a second equation relating β', r and m_C that together with the binding expression enables a simultaneous solution for both r and β' at any given value of m_C. A relatively simple general expression is obtained for r in terms of both m_C and an interaction sum over the charges in the array, which allows r to be determined without explicit knowledge of β'. An equally simple expression relates β' to r, m_C and the interaction sum. The interaction sum is analytically evaluated in the case of a single infinite line of charges and also in the case of two parallel infinite lines of charges. The results obtained for r and β' by using the new auxiliary assumption are identical to those obtained by using the two auxiliary assumptions of the traditional approach in the $m_C \to 0$ limit. However, for each polyion geometry, the results obtained by these two approaches differ substantially at larger values of m_C. (3) It will be explicitly demonstrated that the new alternative assumption predicts qualitatively correct variations of r and β' with m_C. (4) It will be explicitly demonstrated that β' varies with the geometry of an infinite array, even in the limit $m_C \to 0$, by comparing the analytical result for an array of two parallel charged lines, each with axial charge spacing b, with the corresponding result for a single charged line with axial charge spacing $b/2$. (5) We shall evaluate r and β' numerically over a wide range of salt concentration

m_C for isolated, infinite, linearly extended arrays of charges with five different geometries, in each of which every charge is equivalent. (6) The *r*-values predicted for a uniformly charged cylinder by the present theory will be compared with those obtained by solving the non-linear Poisson–Boltzmann equation. As will be seen, the present theory predicts qualitatively correct behavior of *r* for every geometry, and in the case of the uniformly charged cylinder provides a quantitatively useful approximation to the *r*-values obtained from non-linear Poisson–Boltzmann theory. In a second paper, the corresponding binding expressions appropriate for a cylindrical cell model are derived. The computed *r*-values are combined with the Donnan approximation to calculate the osmotic coefficients for various low concentrations of salt in the bathing solution. The resulting *r*-values are comparable to those obtained by combining non-linear Poisson–Boltzmann calculations for zero salt with the Donnan approximation [39], and agree moderately well with recent experimental values [40].

In a third paper, this new approach will be further extended to determine the individual r_j for all charges in an array that may contain inequivalent charges, including arrays of finite extent. As noted above, application of the mean-field, or mean-occupation, approach yields artifactual oscillations in the condensed fraction of counterion charge with position along the polyion. Different approaches to obtain the actual non-oscillatory result will be discussed in that work.

2. Theory for infinite arrays of equivalent charges

2.1. The model

The polyion consists of *N* fixed univalent charges that are not necessarily collinear, but which occupy equivalent positions in a regular array. We focus here on arrays that are linearly extended in one direction. For example, the array might consist of $n>1$ long parallel straight chains symmetrically arranged on the surface of a cylinder, or multi-helix composed of $n>1$ concentric, symmetrically disposed, single-helices. These polyions are so long (i.e. *N* is so large) that end-effects on the average properties are negligible. The intrinsic charges on the isolated chains are regularly spaced so that, when the chains are symmetrically positioned in the array, the charges lie at electrostatically equivalent positions on the surface of a cylinder. A potential binding site for counterions is associated with each intrinsic polyion charge. The salt is present at fixed chemical potential and provides counterions with valence z_C at average concentration m_C and coions (d) with valence z_d at average concentration $|z_C/z_d|m_C$. The polyions also provide sufficient counterions for neutralization of the total polyion charge, but for the solitary polyions considered here that contribution is negligible compared to m_C. Both global and local overcharging are prohibited in the states of lowest energy considered here. Thus, when the polyion is divided into sections, each with $|z_C|$ consecutive univalent sites, no section contains more than a single bound counterion. The maximum number of bound counterions is then $N/|z_C|$, and the condensed fraction of the counterion charge, $r\equiv n_C/(N/|z_C|)$, is the ratio of the actual number of bound counterions per polyion (n_C) to the maximum number of bound counterions, $N/|z_C|$.

2.2. Generic results

When the number (*N*) of intrinsic univalent charges on the polyion is very large, the lattice binding theory described in Appendix A yields the binding relation (Eq. (A19)),

$$r=\beta'|z_C|e^{-1}m_C e^{+2(1-r)L_B|z_C|S_j(\lambda)} \quad (1)$$

where $\beta'=\beta/m_0$ is the (unknown) local effective binding constant for the 1.0 molar standard state, β is the (unknown) local equilibrium constant for the mole fraction 1.0 standard state, $m_0=55.6$ is the molarity of pure liquid water, and m_C is the concentration of the salt, which supplies counterions with valence z_C and coions with valence z_d. Also $L_B=e^2/\varepsilon kT$ is the Bjerrum length, and the interaction sum is defined (with fixed *j*) by

$$S_j(\lambda)\equiv\left(\frac{1}{2}\right)\sum_{l\neq j}e^{-\lambda r_{jl}}/r_{jl}, \quad (2)$$

wherein $\lambda=(8\pi(N_A/1000)(q^2/\varepsilon kT)I)^{1/2}$ is the Debye screening parameter, q is the protonic charge, ε is the dielectric constant, T is the Kelvin temperature, k is Boltzmann's constant, $I=m_C(z_C^2+|z_C/z_d|z_d^2)/2$ is the ionic strength, and r_{jl} is the distance between the jth and lth polyion charges. In deriving Eq. (1) and Eq. (2) it has been assumed that the same condensed fraction of counterion charge, $r_j=r$ is found at all of the equivalent sites of the extremely long polyion. The $S_j(\lambda)$ in Eq. (2) is independent of j, except for a negligible subset of sites near the chain ends.

For completeness we note that Eq. (1) and Eq. (2) apply equally well to non-linear arrays containing equivalent charges in sufficient number, such as a many-sided regular planar polygon or a regular or Archimedean polyhedron with charges at the apices.

For a straight line of discrete charges with uniform spacing b along the polyion, the interaction sum is well known

$$S_j(\lambda)=\sum_{l=1}^{\infty}\frac{e^{-\lambda bl}}{bl}=-\frac{1}{b}\ln(1-e^{-\lambda b}) \tag{3}$$

and

$$r=\beta' e^{-1}|z_C|m_C(1-e^{-\lambda b})^{-2(1-r)(L_B|z_C|/b)} \tag{4}$$

If β' is identified with Manning's free volume, then Eq. (4) becomes identical to the corresponding binding expression of Manning for the same circumstance [4,5]. This single equation was originally 'solved' for the two unknowns, r and β', by first assuming that $d\beta'/dm_C=0$, so β' is constant and does not contribute to the variation of the rhs of Eq. (4) with m_C. In the limit $m_C=0$, and when $L_B|z_C|/b>1.0$, the rhs of Eq. (4) is infinite for $r<1-1/(L_B)|z_C|/b)$ and zero for $r>1-1/(L_B|z_C|/b)$; hence no solution is possible, except when $r=1-1/(L_B|z_C|/b)$, which is adopted as the limiting solution for r. In the limit $m_C=0$, this same value of r satisfies Eq. (4), for any value of β', due to the strength of the singularity. Conversely, any value of β' could in principle satisfy Eq. (4) when $m_C=0$. However, by assuming that $dr/dm_C=0$ in the domain of sufficiently small m_C, one may employ the limiting value of r away from the $m_C=0$ limit but still in the domain of small m_C. Then, the corresponding value of β' is obtained by solving Eq. (4) for some small, but non-vanishing, value of m_C, for which the rhs of Eq. (4) exhibits no true discontinuity. Substituting the limiting value, $r=1-1/(L_B|z_C|/b)$, into the rhs of Eq. (4) renders it independent of m_C, and the subsequent solution for β' gives

$$\beta'=e4\pi b^3(N_{Av}/1000)\times\big((L_B|z_C|/b)-1\big)(1+|z_d/z_C|) \tag{5}$$

where N_{Av} is Avogadro's number. Eq. (5) is identical to Manning's expression for the free volume.

In the protocol suggested by Manning, the extension to finite m_C is effected by assuming that β' remains constant from $m_C=0$ up to moderate m_C. Moreover, it has commonly been assumed that the value of β' in Eq. (5) for discretely charged lines applies also for infinite linearly extended arrays with alternative geometries, such as bundles of two or more parallel discretely charged lines or double-helices. However, both of these assumptions are incorrect, as shown by the following arguments and examples. (1) As noted in the introduction, β' is expected to decrease with increasing m_C, regardless of whether it represents the free volume occupied by the condensed counterions, or instead represents a local effective binding constant. (2) When the Manning protocol is applied to a discretely charged line, Eq. (5) is inserted into Eq. (4) and the latter is then solved for r at various values of m_C. The resulting r-values are predicted to increase with increasing m_C, as shown explicitly for an intrinsic charge spacing $b=3.4$ Å by the open squares in Fig. 1. However, when the salt concentration is sufficiently high that interactions between adjacent polyion charges are negligibly small, no counterion condensation is expected. Consequently, r must actually decrease and vanish at sufficiently large m_C, contrary to the predictions of the Manning protocol! A particular example of this expected decrease in counterion condensation is as follows. Consider an infinitely long uniformly charged cylinder of arbitrary (finite) diameter. First, the non-linear Poisson–Boltzmann equation is solved to obtain the surrounding electrostatic potential for various

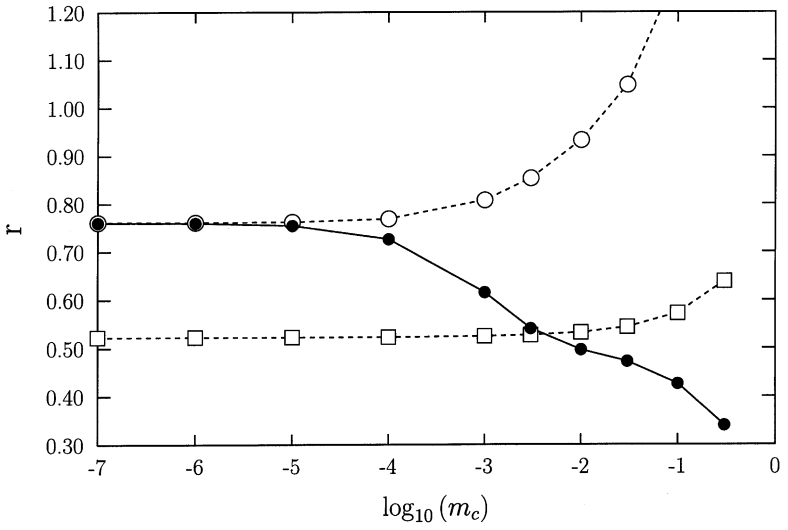

Fig. 1. Comparison of the Manning protocol with the present approach for polyions of infinite length. r vs. $\log_{10} m_C$. r is the condensed fraction of counterion charge and m_C is the concentration of univalent counterions. Open circles (○) are calculated via the Manning protocol for two parallel charged lines, each with axial charge spacing $b=3.4$ Å, that are separated by $d=200$ Å. These calculations are performed by assuming that $\beta'=\beta'_0$ remains fixed at the value given by Eq. (22) adopting Eqs. (15), (16) and (18) for $S_j(\lambda)$, and solving Eq. (1) for r. Open squares (□) are calculated via the Manning protocol for a single charged line with axial spacing $b=3.4$ Å. These calculations are performed by fixing β' at the β'_0 given by Eq. (5), and then solving Eq. (4) for r. Filled circles (●) are the results of the present approach for two parallel charged lines, each with axial spacing $b=3.4$ Å, that are separated by $d=200$ Å. This curve, which also appears in Fig. 2, is calculated using Eq. (20).

ionic strengths. In its linear region, which prevails at a sufficient distance from the cylinder, the nonlinear potential has the same form as the solution of the linear Poisson–Boltzmann equation. By matching the magnitude of the latter to the former, the effective linear charge density required in the linear theory to achieve the match can be determined [1,3]. That effective linear charge density in the linear theory is found to be less than the actual linear charge density of the polyion, and to approach that value with increasing m_C. This will be explicitly demonstrated in Fig. 4 below. Because the difference between the actual charge density and the effective value in the tail-matched linear theory represents the condensed counterion charge, the condensed fraction of the counterion charge manifestly decreases with increasing m_C in this example. The contrary increase in r with increasing m_C that is predicted by the Manning protocol is a direct consequence of the assumption that β' is constant. Any site with an invariant binding constant must proceed monotonically toward saturation with increasing ligand concentration, so r perforce increases with m_C in such a case. However, counterion condensation at finite m_C behaves differently, in a manner much more closely approximated by the present alternative approach as will be demonstrated explicitly below. (3) The effective binding constant β' generally depends upon the lateral geometry of the array as well as on the axial charge spacing, even when $m_C=0$, as demonstrated explicitly below for the case of two parallel discretely charged lines. In the $m_C=0$ limit the same value of β' should, and can, be obtained under either the original assumptions of the Manning protocol, namely $d\beta'/dm_C=0$ and $dr/dm_C=0$, or under the alternative assumption described below, because they are equivalent in that case. However, in most previous applications of the Manning protocol it was not noticed that β' varies with lateral geometry of the array, and Eq. (5) was simply used for all geometries. When this oversight is rectified, β' is found to vary with lateral geometry of the array even within

the Manning protocol [30]. In either the Manning protocol or in the present alternative protocol (described below) the value of β' affects the condensed fraction r only at finite m_C when r begins to deviate from its limiting value. (4) In the case of two parallel charged lines, as m_C increases beyond the point where the two lines no longer significantly interact, both β' and r must decrease from the values characteristic of the two parallel lines to the values typical of the corresponding single charged lines. However, when the Manning protocol with the constant value of β' appropriate for two parallel charged lines is applied, it again predicts an increase in r with increasing m_C, contrary to expectation. Explicit results of the Manning protocol for the case of two parallel charged lines, each with intrinsic charge spacing $b=3.4$ Å, separated by $d=200$ Å, are given by the open circles in Fig. 1. Neither the expected decrease in r nor the expected merging of the curve of open circles with that of the open squares (typical of each constituent single charged line) is observed. This is a clear demonstration that the Manning protocol for extending counterion condensation theory to finite m_C is invalid. As will be seen, these errors arise primarily from the assumption that $d\beta'/dm_C=0$, and can be removed by invoking an alternative assumption to obtain the required auxiliary equation.

2.3. The new auxiliary equation and general results

In order to determine r and β' as a function of m_C, it is generally necessary to invoke a second equation in addition to Eq. (1). We rewrite Eq. (1) as

$$\Delta(r,\beta',m_C)=0 \tag{6}$$

where

$$\Delta(r,\beta',m_C)\equiv r-\beta'|z_C|e^{-1}m_C e^{2(1-r)L_B|z_C|S_j(\lambda)} \tag{7}$$

is the difference between the left and rhs of Eq. (1). $\Delta(r, \beta', m_C)$ is assumed to be a continuous function of its three arguments for $m_C>0$. In view of Eq. (6), its total derivative with respect to m_C must vanish for all m_C:

$$\left(\frac{\partial\Delta}{\partial m_C}\right)_{r,\beta'}+\left(\frac{\partial\Delta}{\partial r}\right)_{\beta',m_C}\left(\frac{dr}{dm_C}\right)+\left(\frac{\partial\Delta}{\partial\beta'}\right)_{r,m_C}\left(\frac{d\beta'}{dm_C}\right)=0 \tag{8}$$

In order to obtain an auxiliary expression from Eq. (8) it is necessary to invoke at least one additional assumption. In the protocol proposed by Manning it was assumed that $d\beta'/dm_C=0$ for all m_C and also that $dr/dm_C\cong 0$ for small m_C, which in view of Eq. (8) implies that $(\partial\Delta/\partial m_C)_{r,\beta'}=0$ for small m_C. In Manning's approach, dr/dm_C and $(\partial\Delta/\partial m_C)_{r,\beta'}$ no longer vanish outside the domain of small m_C. As noted above, this assumption that $d\beta'/dm_C=0$ is incorrect and yields demonstrably invalid results at finite m_C. Hence, we infer that β' must vary, specifically β' must decrease, with increasing m_C. Unfortunately, β' cannot be independently assessed without solving both the nonlinear and linear Poisson–Boltzmann equations for the array of polyion charges. If one could always do that there would be no need for counterion condensation theory. Within the framework of counterion condensation theory one must resort to one or more assumptions that are not well justified in terms of a priori physical/theoretical considerations, but instead in terms of their plausibility and the qualitative correctness and quantitative utility of the resulting predictions.

We propose here an alternative auxiliary assumption, namely that $(\partial\Delta/\partial m_C)_{r,\beta'}=0$ for all m_C. This assumption is neither more nor less arbitrary than those adopted previously, especially the assumption that $d\beta'/dm_C=0$ for all m_C. Moreover, it is actually somewhat less restrictive than the two assumptions that were employed in the Manning protocol in the domain of small m_C, because (in view of Eq. (8)) it requires only that $dr/dm_C=-d\beta'/dm_C[(\partial\Delta/\partial\beta')_{r,m_C}/(\partial\Delta/\partial r)_{\beta',m_C}]$ without further specifying that $dr/dm_C\cong 0$ and $d\beta'/dm_C=0$ separately in that region. In the domain of small m_C, the two assumptions of the Manning protocol, namely $dr/dm_C\cong 0$ and $d\beta'/$

$dm_C = 0$, imply the alternative assumption, $(\partial\Delta/\partial m_C)_{r,\beta'} = 0$, but the converse is not true.

Although this alternative assumption has as yet no rigorous physical justification, it is in a practical sense the only available option within counterion condensation theory. The basic idea is that we would like to determine r and β' by simultaneously solving both $\Delta(r, \beta', m_C) = 0$ and $\Delta(r + (dr/dm_C)dm_C, \beta' + (d\beta'/dm_C)dm_C, m_C + dm_C) = 0$, which are different versions of Eq. (8), for some small, but otherwise arbitrary, value of dm_C. The problem in doing this obviously stems from the unknown variation of r and β' with m_C. The new assumption that $(\partial\Delta(r, \beta', m_C)/\partial m_C)_{r,\beta} = 0$ means that $\Delta(r, \beta', m_C)$ remains invariant to first order small changes in m_C not only when r and β' vary in the correct way, but also when r and β' remain fixed at their starting values, which satisfy $\Delta(r, \beta', m_C) = 0$. According to Eq. (8), this assumption effectively couples the slopes dr/dm_C and $d\beta'/dm_C$ so that the combined slope terms make no net contribution to the total change in $\Delta(r, \beta', m_C)$ with m_C for small dm_C. In any case, under this assumption the same value is obtained for both $\Delta(r, \beta', m_C + dm_C) = 0$ and for $\Delta(r + (dr/dm_C)dm_C, \beta' + (d\beta'/dm_C)dm_C, m_C + dm_C) = 0$. In principle, $\Delta(r, \beta', m_C + dm_C) = 0$ and $\Delta(r, \beta', m_C) = 0$ can then be simultaneously solved to obtain both r and β' which apply to m_C. In the absence of any additional information or assumptions about the separate values of dr/dm_C and $d\beta'/dm_C$, a simultaneous solution for r and β' at arbitrary m_C is possible if, and only if, this alternative assumption is invoked. Thus, within the framework of counterion condensation theory, which affords no independent information about the separate magnitudes of dr/dm_C and $d\beta'/dm_C$, this alternative assumption is really the only avenue open. Its validity should be judged by the qualitative correctness and quantitative accuracy of its predictions, which will be examined below.

The new auxiliary assumption is implemented by differentiating both sides of Eq. (6) with respect to m_C while holding r and β' constant, which gives

$$0 = \tilde{\beta} e^{2(1-r)L_B|z_C|S_j(\lambda)} + m_C\tilde{\beta}\big(2(1-r)L_B|z_C|\big) \times \frac{\partial S_j(\lambda)}{\partial\lambda}\,\frac{d\lambda}{dm_C}\, e^{2(1-r)L_B|z_C|S_j(\lambda)} \quad (9)$$

where $\tilde{\beta} \equiv \beta' e^{-1}|z_C|$. After multiplying Eq. (9) by m_C, inserting $d\lambda/dm_C = (K/2)m_C^{-1/2}$, where

$$K \equiv [8\pi(N_A/1000) \times (q^2/(\varepsilon kT))(1/2)(z_C^2 + |z_C/z_d|z_d^2)]^{1/2},$$

and making use of Eq. (1), there results

$$0 = r + r(1-r)m_C^{1/2}KL_B|z_C|\frac{\partial S_j(\lambda)}{\partial\lambda} \quad (10)$$

The $r = 0$ solution applies only when no counterion condensation occurs. When $r \neq 0$, the common r factors may be divided out to obtain

$$r = 1 - \frac{1}{[m_C^{1/2}KL_B|z_C|(-)\partial S_j(\lambda)/\partial\lambda]} \quad (11)$$

β' can be found by substituting this value of r into Eq. (1), which is rewritten as

$$\beta' = \frac{er}{(m_C|z_C|e^{2(1-r)L_B|z_C|S_j(\lambda)})} \quad (12)$$

Eqs. (11) and (12) are the principal generic results of this section. In this formulation, r can be found from Eq. (11) without knowledge of β'. The sum in Eq. (11) can be evaluated either by numerical differentiation of $S_j(\lambda)$, or by directly evaluating the sum,

$$(-)\frac{\partial S_j(\lambda)}{\partial\lambda} = \sum_{j=1}^{\infty} e^{-\lambda r_{jl}} \quad (13)$$

3. Specific results and discussion

Numerical values of r and β' are now calculated for five different linear arrays of infinite extent over a range of m_C from 10^{-7} to 0.3 M. All numerical calculations are performed for a uni-univalent salt ($|z_C| = 1 = |z_d|$), $T = 293$ K, and a dielectric constant $\varepsilon = 80.0$, so that $K = 3.28332 \times 10^7\ \mathrm{cm^{-1}\,M^{-1/2}}$. All of the calculations using counterion condensation theory were performed using Mathematica 4. Analytical results for

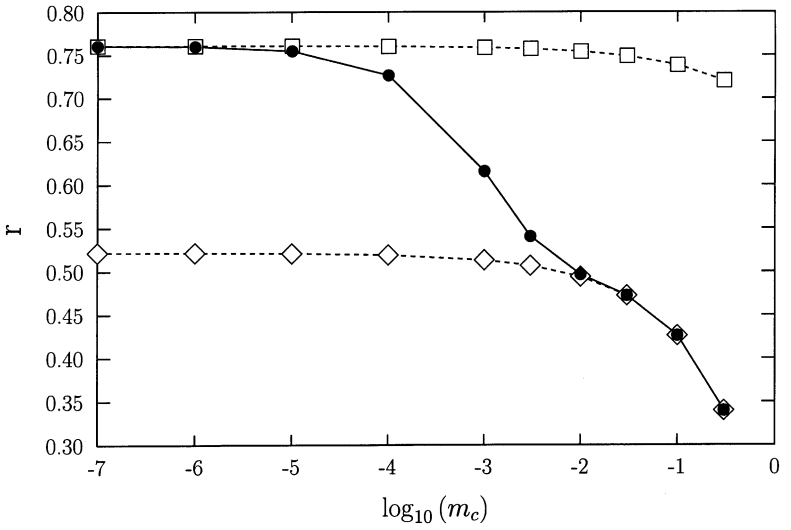

Fig. 2. r vs. $\log_{10} m_C$ for different polyions of infinite length. r is the condensed fraction of counterion charge and m_C is the concentration of univalent counterions. Open squares (□) apply for a single line of charges with axial spacing $b=1.7$ Å. Open diamonds (◇) apply for a single line of charges with axial spacing $b=3.4$ Å. Filled circles (●) apply for two parallel lines of charges, each with axial spacing $b=3.4$ Å, that are separated by $d=200$ Å. Open symbols are calculated using Eq. (14) and the filled symbols using Eq. (20), both of which are special cases of Eq. (11) of the present alternative approach.

the array consisting of two infinite parallel lines of charges are also presented.

3.1. A single infinite line of charges with uniform spacing b

In this case, $S_j(\lambda)$ is given by Eq. (3), and Eq. (11) becomes:

$$r=1-m_C^{-1/2}(KL_B)^{-1}(e^{\lambda b}-1) \qquad (14)$$

In the limit $m_C\to 0$, we have $e^{\lambda b}-1\cong\lambda b=Kbm_C^{1/2}$, and $r_0=1-1/(L_B/b)$, which is the Manning result [4,5]. Use of this value of r_0 in the same $m_C\to 0$ limit in Eq. (12) yields β'_0, which is precisely the Manning value of β' in Eq. (5) as expected.

Eqs. (14) and (12) are numerically evaluated to yield the appropriate values of r and β' for this single charged line at finite m_C. For an axial (or longitudinal) spacing, $b=3.4\times10^{-8}$ cm, the corresponding values of r are presented in Figs. 2 and 3, and the corresponding β' values are given in Table 1. The condensed fraction r remains relatively constant near its low-salt limiting value, 0.522, for $m_C\lesssim 3\times10^{-3}$ M, but declines significantly at higher m_C, especially when $m_C\gtrsim 10^{-2}$ M, where $\lambda b\gtrsim 0.1$. Similar calculations are performed for a 2-fold smaller longitudinal charge spacing, $b=1.7\times10^{-8}$ cm, and the corresponding r-values are plotted in Figs. 2 and 3 and the β' values are presented in Table 1. In this case, r remains near its low-salt limiting value, $r_0=0.761$, for $m_C\lesssim 0.1$ M, but declines significantly at higher m_C, especially when $m_C\gtrsim 0.3$ M, where $\lambda b\gtrsim 0.3$. In both cases, namely when $b=3.4\times10^{-8}$ and $b=1.7\times10^{-8}$ cm, with increasing m_C, β' descends significantly below its limiting value before r declines appreciably. It is noteworthy that the steep relative decline in r sets in at a much smaller value of λb for the chain with $b=3.4$ Å than for that with $b=1.7$ Å. That is, the onset of the decline in r does not scale exactly with λb, which is not too surprising, since there are three different relevant length scales, namely b, L_B and λ^{-1}, and two relevant dimensionless ratios, λb and λL_B, in this problem.

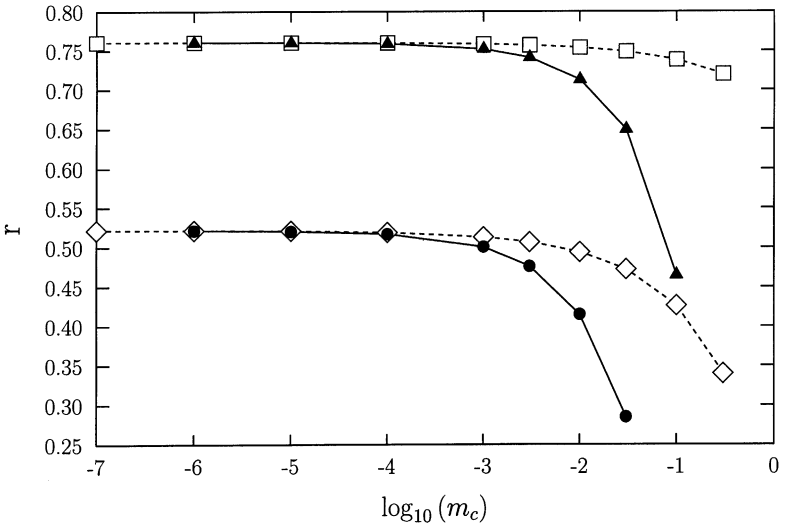

Fig. 3. r vs. $\log_{10} m_C$ for different polyions of infinite length. r is the condensed fraction of counterion charge and m_C is the concentration of univalent counterions. Filled circles (●) apply for a single-helix with diameter $d=20$ Å and 10 charges per turn with axial spacing $b=3.4$ Å. Filled diamonds (♦) apply for a double-helix that consists of two identical concentric single helices, each with diameter $d=20$ Å and 10 charges per turn with axial spacing $b=3.4$ Å. The second helix is rotated by π about the helix axis from a position of coincidence with the first. Open diamonds (◇) apply for a single charged line with axial spacing $b=3.4$ Å. This same curve appeared also in Fig. 2. Open squares (□) apply for the single charged line with axial spacing $b=1.7$ Å. This same curve also appeared in Fig. 2.

Table 1
Values of β' for different models

m_C (M)	β'_I (M^{-1})[a]	β'_{II} (M^{-1})[b]	β'_{III} (M^{-1})[c]	β'_{IV} (M^{-1})[d]	β'_V (M^{-1})[e]
10^{-7}	1.712	0.624	131.287	n.c.[f]	n.c.[f]
10^{-6}	1.710	0.624	127.247	19.46	30.67
10^{-5}	1.691	0.622	106.549	19.23	30.53
10^{-4}	1.629	0.611	50.742	18.23	29.50
10^{-3}	1.473	0.580	6.332	14.86	25.38
3×10^{-3}	1.343	0.552	2.062	11.72	21.27
10^{-2}	1.147	0.507	1.179	7.26	15.12
3×10^{-2}	0.919	0.457	0.920	3.11	8.99
10^{-1}	0.630	0.372	0.630	n.s.[g]	3.33
3×10^{-1}	0.356	0.287	0.356	n.s.[g]	n.s.[g]

[a] Computed for a single-line of discrete charges with axial charge spacing $b=3.4\times10^{-8}$ cm.

[b] Computed for a single-line of discrete charges with axial charge spacing $b=1.7\times10^{-8}$ cm.

[c] Computed for two parallel lines of discrete charges separated by $d=200\times10^{-8}$ cm, each with axial charge spacing $b=3.4\times10^{-8}$ cm.

[d] Computed for a single-helix of discrete charges with diameter $d=20\times10^{-8}$ cm, axial charge spacing $b=3.4\times10^{-8}$ cm, and helix succession angle $\phi=2\pi/10$.

[e] Computed for a double-helix of discrete charges with diameter $d=20\times10^{-8}$ cm, axial charge spacing $b=3.4\times10^{-8}$ cm on each constitute single-helix, and helix succession angle $\phi=2\pi/10$.

[f] n.c., not calculated, due to inadequate convergence.

[g] n.s., negative solution for r at this value of m_C implies that $r=0$, and no solution exists for β'.

The values of r and β' predicted by this alternative protocol both decline with increasing m_C, as expected on physical grounds. In these regards, the predictions of the alternative protocol are at least qualitatively correct.

3.2. Two parallel infinite lines of in-phase uniformly spaced charges

In this case, the interaction sum is divided into two subsums. The first sum contains all interactions between the jth charge on one line and all other charges on the same line, whereas the second subsum contains all interactions between the jth charge on one line and all charges on the second parallel line. That is,

$$S_j(\lambda) = S_{j1}(\lambda) + S_{j2}(\lambda), \tag{15}$$

where

$$S_{j1}(\lambda) \equiv \sum_{l=1}^{\infty} \frac{e^{-\lambda b l}}{bl} = -\frac{1}{b}\ln(1-e^{-\lambda b}) \tag{16}$$

which is just the result in Eq. (3), and

$$S_{j2}(\lambda) = \frac{1}{2}\frac{e^{-\lambda d}}{d} + \sum_{l=1}^{\infty} \frac{e^{-\lambda r_{jl}}}{r_{jl}} \tag{17}$$

where $r_{jl} \equiv (d^2 + (bl)^2)^{1/2}$ is the distance from the jth charge on one line to the lth charge on the second line, which is longitudinally displaced by a distance bl and laterally displaced by d. S_{j2} can be readily evaluated numerically at finite m_C. However, when $d \gg b$, as will be assumed here, $S_{j2}(\lambda)$ can be accurately approximated by using the linear Poisson–Boltzmann electrostatic potential for a uniformly charged line with linear charge density $(1-r)q/b$, namely $\psi(d) = [(1-r)q/\varepsilon b]2K_0(\lambda d)$, and the corresponding electrostatic free energy of a line element (b) with charge $(1-r)q$ placed in the electrostatic potential arising from the other line, namely, $A_{j2} = [(1-r)^2q^2/\varepsilon b](1/2)(2)K_0(\lambda d) = [(1-r)^2q^2/\varepsilon]S_{j2}$, which gives

$$S_{j2}(\lambda) = (1/b)K_0(\lambda d) \tag{18}$$

where $K_0(\lambda d)$ is the 0th order modified Bessel function. In this case,

$$\frac{\partial S_j(\lambda)}{\partial \lambda} = -\frac{1}{(e^{\lambda b}-1)} - \frac{d}{b}K_1(\lambda d) \tag{19}$$

and

$$r = 1 - m_C^{-1/2}(KL_B)^{-1}\left\{(e^{\lambda b}-1)^{-1} + (d/b)K_1(\lambda d)\right\}^{-1} \tag{20}$$

where $K_1(x) = -dK_0(x)/dx$ is the first order modified Bessel function, and

$$\beta' = \frac{re(1-e^{-\lambda b})^{2(1-r)L_B/b} e^{-2(1-r)(L_B/b)K_0(\lambda d)}}{m_C} \tag{21}$$

In the limit $m_C \to 0$, we have $e^{\lambda b} - 1 \cong \lambda b = Kbm^{1/2}{}_C$, $K_1(\lambda d) \cong +1/(Kdm_C^{1/2})$, and $r_0 = 1 - 1(L_B/(b/2))$, as expected for a linear array with an average axial charge spacing, $b/2$. In the domain of very small m_C, $K_0(\lambda d) \to -\{\ln(\lambda d/2) + \gamma\}$, where $\gamma = 0.5772$ is the Euler–Mascheroni constant, and

$$\beta'_0 = e^{1+\gamma} 8\pi (N_A/1000)(L_B/b - 1/2)b^2 d/2 \tag{22}$$

Eq. (22) demonstrates clearly that β' (or the free volume) depends on the 'structure' of the linear array (via its dependence upon d), as well as its linear charge density, even in the zero salt ($m_C = 0$) limit. These results for r_0 and β'_0 in the $m_C \to 0$ limit are identical to the corresponding results that are obtained by using the protocol of Manning, [4,5] because the two assumptions employed in that protocol in the $m_C \to 0$ limit, namely $\partial r/\partial m_C \cong 0$ and $\partial \beta'/\partial m_C = 0$ imply the present assumption, $(\partial \Delta/m_C)_{r,\beta'} = 0$ and are equivalent to it in that limit.

Eqs. (20) and (21) are numerically evaluated at finite m_C to yield the appropriate values of r and β' for the case of two parallel charged lines separated by a distance $d = 200 \times 10^{-8}$ cm, each with longitudinal charge spacing $b = 3.4 \times 10^{-8}$ cm. The corresponding values of r are presented

in Figs. 1 and 2, and the values of β' are displayed in Table 1. At low values of $m_C \lesssim 10^{-6}$ M, r remains quite close to the limiting value at $m_C = 0$, namely $r_0 = 0.761$, which is identical to that of a single straight chain with $b = 1.7 \times 10^{-8}$ cm, but descends steeply between $m_C = 10^{-4}$ and 10^{-2} M to a shelf that lies near the limiting value characteristic of the single constituent charged lines, each with $b = 3.4 \times 10^{-8}$ cm, namely $r_0 = 0.523$. β' behaves in a qualitatively similar fashion, but its transition between the values characteristic of 2 chains and 1 chain is considerably broader. Indeed, already at $m_C = 10^{-7}$ M, $\beta' = 131.287$ lies significantly below the limiting value, $\beta'_0 = 134.969$ calculated via Eq. (22) The value of r is about mid-way through the transition, when $m_C \cong 10^{-3}$ M, at which point $\lambda d \cong 2.0$, and the two lines are significantly screened from one another. This transition of r for the two parallel charged lines from values characteristic of a single charged line with $b = 1.7 \times 10^{-8}$ cm at low m_C to those typical of a single charged line with $b = 3.4 \times 10^{-8}$ cm at higher m_C (cf. Figs. 2 and 3) is a clear demonstration of the important effect of local structure on counterion condensation at finite m_C.

3.2.1. Comparison with results of the Manning protocol at finite m_C

When the original assumptions and protocol of Manning are applied to the case of two parallel discretely charged lines, each with $b = 3.4$ Å, which are separated by $d = 200$ Å, in the $m_C \to 0$ limit, the values of r_0 and β'_0 obtained are identical to those found via the present alternative approach. However, with increasing m_C in the region $m_C \gtrsim 10^{-4}$ M where $\lambda d \gtrsim 0.7$, the Manning protocol (wherein $\beta' = \beta'_0$ for all m_C) predicts an increase in r above the limiting value, $r_0 = 0.761$, as shown by the open circles in Fig. 1, whereas the present treatment predicts a decrease in r from $r_0 = 0.761$ down to approximately $r = 0.5$, where the curve for the two parallel lines merges with that for either single line (c.f. Fig. 2). This merging of the two curves is absolutely required, whenever λd is so large that the individual lines no longer interact with one another. The Manning protocol clearly fails to capture this essential aspect of the expected behavior.

3.3. A single-helix of discrete charges with uniform axial spacing

In this case, the helix diameter is d, and there are exactly 10.0 charges per turn with a longitudinal separation (axial spacing) b between them. The interaction sum in Eq. (2) becomes (with fixed j)

$$S_j(\lambda) = \sum_{l=1}^{\infty} \frac{e^{-\lambda r_{jl}}}{r_{jl}} \tag{23}$$

where

$$r_{jl} = \left[(lb)^2 + (d\sin(l\phi/2))^2\right]^{1/2} \tag{24}$$

and $\phi = 2\pi/10.0$ is the helix succession angle between neighboring charges. Although analytical evaluations were not achieved in this case, numerical evaluations of $S_j(\lambda)$ were performed over the range of m_C from 10^{-6} to 0.03 M by evaluating the sum up to an upper limit of $l = 10\,000$, at which point the interaction sum was satisfactorily converged in every case considered. The slope was evaluated numerically according to

$$\frac{\partial S_j(\lambda)}{\partial \lambda} = \frac{S_j((1.001)\lambda) - S_j(\lambda)}{(0.001)\lambda} \tag{25}$$

Results obtained using Eq. (25) match those from Eq. (13)

The calculated values of r and β' for this single-helix with $d = 20 \times 10^{-8}$ cm and $b = 3.4 \times 10^{-8}$ cm are presented in Fig. 3 and Table 1, respectively. At low-salt concentration, $m_C \leqslant 10^{-3}$ M, r lies very close to the values predicted for a single straight line with the same axial spacing between charges, but at higher values of m_C, r for the single-helix falls progressively farther below that for the straight line. This is due to the lateral 'structure' of the helix wherein the charges are farther apart and the electrostatic interactions between neighboring charges are more screened than in the case of the straight line. At all values of m_C, β' for the single-helix significantly exceeds the corresponding value for the straight line with

the same axial spacing between charges. As in the case of two parallel lines, local structure of the single-helix affects β′ even at very low values of m_C, as noted recently by Manning 50.

3.4. A double-helix of discrete charges with uniform axial spacing of pairs of charges

We consider a double-helix that consists of two identical concentric single helices of the same kind as in the previous section. That is, each single-helix has diameter d and 10.0 charges per turn with an axial (longitudinal) spacing b between them. The second helix is rotated by π about the symmetry axis of the double-helix from a position of coincidence with the first helix. The succession angle of both single and double helices is $\phi = 2\pi/10.0$, and the helix repeat distance is 10 b per turn. Along the direction of the helix axis, the charges of the double-helix occur in pairs (one charge on each single-helix), one pair every axial spacing b. Hence, the average axial spacing per ionic charge on the double-helix is $b/2$. As in the case of the two parallel straight lines, the interaction sum (with fixed j) can be decomposed into two subsums,

$$S_j(\lambda) = S_{j1}(\lambda) + S_{j2}(\lambda) \tag{26}$$

where $S_{j1}(\lambda)$ contains the interactions of the jth charge with all other polyion charges on the same helix, and $S_{j2}(\lambda)$ contains its interactions with all charges on the opposite helix. Indeed, $S_{j1}(\lambda)$ is given precisely by Eq. (22) and Eq. (23) above and

$$S_{j2}(\lambda) = \frac{1}{2}\,\frac{e^{-\lambda d}}{d} + \sum_{l=1}^{\infty} \frac{e^{-\lambda \tilde{r}_{jl}}}{\tilde{r}_{jl}} \tag{27}$$

where

$$\tilde{r}_{jl} = \left\{ (lb)^2 + (d/2)^2 \left[(\cos(l\phi + \pi) - 1)^2 + (\sin(l\phi))^2 \right] \right\}^{1/2} \tag{28}$$

is the distance between the jth charge on the first helix and the lth charge on the opposite helix. The latter charges are indexed by the integer l, which is set to $l = 0$ at the axial position corresponding to the jth charge on the first helix. The quantity in square brackets can be simplified to $4\cos^2(l\phi/2)$, if desired. $S_{j1}(\lambda)$ and $S_{j2}(\lambda)$ are evaluated numerically to satisfactory accuracy over the range of m_C from 10^{-6} to 0.10 M by summing to $l = 10\,000$, at which point the interaction sums were adequately converged in each case. The slopes of $S_{j1}(\lambda)$ and $S_{j2}(\lambda)$ were both calculated numerically according to Eq. (25).

The calculated values of r and β′ for this double-helix with $d = 20 \times 10^{-8}$ cm and $b = 3.4 \times 10^{-8}$ cm are presented in Fig. 3 and Table 1, respectively. This model corresponds approximately to the charge array of a straight DNA. As can be seen in Fig. 2, the double-helix with diameter $d = 20 \times 10^{-8}$ cm exhibits practically the same values of r at low m_C as are found for the single charged line with $b = 1.7 \times 10^{-8}$ cm, and for the array of two parallel charged lines that are separated by $d = 100 \times 10^{-8}$ cm, but together have the same average axial spacing between charges as the double-helix, namely $b/2 = 3.4 \times 10^{-8}/2 = 1.7 \times 10^{-8}$ cm. This demonstrates the expected invariance of r to local geometry for the same average axial charge spacing at very low m_C. At larger $m_C \gtrsim 10^{-3}$ M r for the two parallel charged lines declines, as the two lines become effectively screened from one another. However, the two helices of the double-helix do not become significantly screened until $m_C \gtrsim 10^{-2}$ M due to the close proximity of the nearest charges on one helix to any given charge on the opposite helix. For this double-helix, r is predicted to fall to zero for m_C between 0.1 and 0.3 M. Values of β′ for the double-helix exceed the corresponding values for the single-helix and those for either single charged line, again demonstrating the dependence of β′ on local structure.

The helical array of charges modeled here is similar to duplex DNA in regard to helix diameter, pitch, and axial charge spacing (or linear charge density). The present results suggest that use of the limiting value, $r = 0.761$, which is appropriate for $m_C = 0$, for counterion concentrations that equal or exceed 10^{-2} M may lead to significant error in the case of duplex DNA.

3.5. A cylindrical array of parallel charged lines

We consider m parallel, infinite, discretely charged, straight lines that are uniformly disposed in a cylindrical array. Since our objective is to model a uniformly charged cylinder with diameter of DNA ($d=20$ Å), we take many charged lines ($m=100$). We also want each line to appear continuously charged as viewed by every other line, so the spacing of discrete charges on each line is taken to be b/n, where $b=1.7$ Å is the average axial spacing between full phosphate charges of DNA and $n=1000$. The distance between neighboring lines, $d\sin(2\pi/2(100))=6.28\times10^{-9}$ cm exceeds the distance between charges on any given line, $b/1000=1.7\times10^{-11}$ cm, by 370-fold. Moreover, the Debye screening length of the highest ionic strength considered exceeds the distance between lines by 13-fold. We wish our 'cylinder' to have the same linear charge density as DNA, which in view of the preceding remarks means that the elementary charges q in our array must be much smaller than the electronic charge, specifically $q=e/(m{\cdot}n)$. The electrostatic energy in Eq. (A17) is reformulated in terms of the new charge, $q=e/(mn)$ and the new total number of charges in the polyion, Nmn, and an interaction sum over all of the new charges. The final result is that an additional factor, $1/(mn)$, appears in the exponents of Eq. (A19) and Eq. (1). Upon applying the auxiliary condition there results

$$r=1-\frac{1}{m_C^{1/2}KL_B\big(|z_C|/(mn)\big)\big(-\partial S_{j1}/\partial\lambda-\partial S_{j2}/\partial\lambda\big)} \tag{29}$$

where

$$S_{j1}(\lambda)=-(1/(b/n))\ln\big(1-e^{-\lambda/(b/n)}\big) \tag{30a}$$

$$S_{j2}(\lambda)=\sum_{l=1}^{m-1}(1/(b/n))K_0(\lambda d_l) \tag{30b}$$

and $d_l=d|\sin(2\pi l/(2m))$ is the distance between any given line and its lth neighbor counting sequentially around the cylinder. Inserting the corresponding analytical expressions from Eq. (19) yields finally

$$r=1-\frac{1}{m_C^{1/2}KL_B\big(|z_C|/(mn)\big)\left(\big(e^{\lambda b/n}-1\big)^{-1}+\sum_{l=1}^{m-1}(d_l/(b/n))K_1(\lambda d_l)\right)} \tag{31}$$

The corresponding expression for β' is readily obtained but is not of interest in this case.

In the limit $m_C\to0$, $(e^{\lambda(b/n)}-1)^{-1}\to1/(\lambda b/n)$ and $(d_l/(b/n))K_1(\lambda d_l)\to1/\lambda(b/n)$, so $r=1-1/(L_B|z_C|/b)$. In the present case of uni-univalent salt, $|z_C|=1.0$, and $r_0=1-1/(L_B/b)$, which is the same as for a single line of electronic charges (e) with spacing b, as expected.

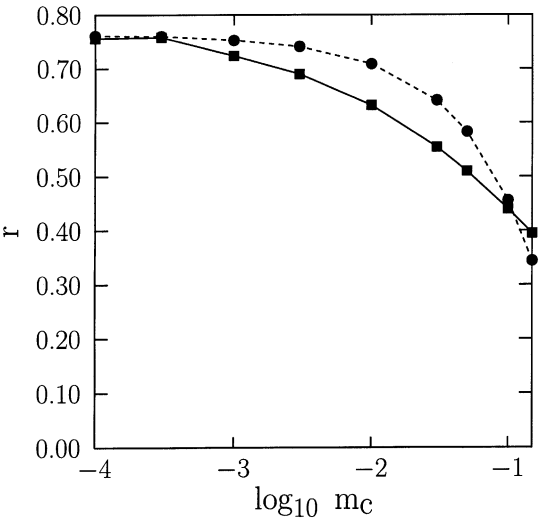

Fig. 4. r vs. $\log_{10} m_C$ for a uniformly charged infinite cylinder with the diameter ($d=20$ Å) and linear charge density ($\nu_{DNA}=-|e|/(1.7$ Å)) of DNA. r is the condensed fraction of polyion charge and m_C is the concentration of univalent counterions. Filled circles (●) are calculated according to the present counterion condensation theory via Eq. (31), as described in the text. Filled squares (■) are calculated by solving the non-linear Poisson–Boltzmann (NLPB) equation, determining the effective linear charge density, ν_{eff}, that in the linear theory yields the same potential as the NLPB solution in the very tail of the latter, and reckoning the condensed fraction of charge as: $r=(\nu_{DNA}-\nu_{eff})/\nu_{DNA}$. $T=293$ K, and $\varepsilon=80$.

The condensed fraction is evaluated numerically for a range of salt concentrations from 10^{-4} to 0.15 M, and the results are presented in Fig. 4. In 10^{-4} M salt, the condensed fraction of counterion charge, $r=0.758$, is close to the Manning limit, $r_0=0.761$. At higher salt concentrations r decreases, and follows very closely the corresponding curve for the double-helix with the same diameter and linear charge density in Fig. 3 (not shown).

3.5.1. Comparison with non-linear Poisson–Boltzmann theory

Also shown in Fig. 4 are the corresponding r-values calculated from non-linear Poisson–Boltzmann theory for a uniformly charged cylinder, as described by Delrow et al. [3]. In this case, r is calculated by taking the difference between the actual polyion charge per unit length (ν_{act}) and the effective charge per unit length (ν_{eff}) that enables the solution of the linearized (Debye–Hückel) Poisson–Boltzmann equation to precisely match that of the non-linear Poisson–Boltzmann equation in the linear 'tail' region of the latter, and then dividing this difference by ν_{act}. That is,

$$r \equiv (\nu_{act} - \nu_{eff})/\nu_{act} \quad (32)$$

Our protocol follows that implemented by Sugai and Nitta [41], which yields the effective charge of the tail-matching Debye–Hückel theory in the most direct and unequivocal manner. The results of the non-linear Poisson–Boltzmann theory are co-plotted with those of the present counterion condensation theory in Fig. 4. The present theory agrees closely with non-linear Poisson–Boltzmann theory at salt concentrations at or below 0.0003 M, and again at 0.1 M, and deviates only modestly ($\leqslant 15\%$) over the entire range from 0.0003 to 0.15 M. If this level of accuracy should apply to other charged arrays of comparable diameter, then the present extension of counterion condensation theory would be quantitatively useful, especially for finite irregular arrays of discrete charges, for which solutions of the non-linear Poisson–Boltzmann equation and Monte Carlo simulations are still somewhat impractical. The results of the counterion condensation theory in Fig. 4 are invariant to a 10-fold reduction in the number of parallel lines that constitute the cylinder and a simultaneous 10-fold reduction in the charge spacing along each line, provided the diameter and linear charge density remain unaltered. This demonstrates that the density of discrete charges is sufficiently high to satisfactorily simulate a uniformly charged cylinder up to the highest ionic strength considered (0.15 M).

An important feature of both curves in Fig. 4 is the decline of the condensed fraction with increasing salt concentration, which is due to the screening of electrostatic interactions between any given charge and those on the opposite side of the cylinder. Interestingly, the discrepancy between the two curves is maximal (in the range considered), when the salt concentration is approximately 0.03 M and $\lambda d \cong 1.0$.

It is not known to what extent, if any, the modest discrepancy in r-values predicted by the counterion condensation and non-linear Poisson–Boltzmann theories arises from the difference in models. The counterion condensation theory pertains to a porous cylinder, in which the counterions have full access to the interior of the rod, whereas the non-linear Poisson–Boltzmann theory pertains to an impermeable cylinder. Since it is not apparent how to extend counterion condensation theory to treat impermeable arrays of charges and since the interiors of many polyions are impermeable to counterions, the present comparison may be the most relevant in any case. The results demonstrate clearly that the present counterion condensation theory yields fairly approximate results in the salt regime from 0.0003 to 0.15 M. Nevertheless, the modest size of the discrepancy suggests that the present theory may provide a quantitatively useful approximation to the condensed fraction in this regime for alternative geometries, where the non-linear Poisson–Boltzmann equation is not so readily solved.

3.6. Comparison with previous studies

The spatial envelope of the Manning fraction of condensed counterions and its variation with counterion concentration have been investigated via non-linear Poisson–Boltzmann theory and Monte Carlo simulations [17,31,32]. Partial invasion of

this envelope by neutral salt occurs when the external salt concentration is increased, and leads to an increase in counterions within this domain. This has sometimes been interpreted as an increase in the condensed fraction of counterions with increasing salt concentration. However, the presence of coions in equal-charge amounts within the same domain insures that the actual compensating charge within the envelope occupied by the Manning fraction (or any other fraction) of the counterion charge does not change with increasing salt concentration. That is, after the counterions attributable to the invading neutral salt are subtracted out, there remains only the Manning fraction. In this work, the magnitude of the condensed fraction is defined in a rather different way, according to Eq. (32) The variation in magnitude of the condensed fraction of counterion charge, as defined here, with increasing counterion concentration has not been investigated previously via solutions of the non-linear Poisson–Boltzmann equation.

3.7. Summary of results

The above results for infinite arrays of equivalent charges predict that the effective binding constant β' (or the free volume) declines with increasing m_C over the relevant concentration ranges, as expected, and also varies substantially with polyion structure, generally increasing with the number of chains and lateral dimension of the charged array, also as expected. Thus, our proposed assumption that $(\partial\Delta(r, \beta', m_C))_{r,\beta'}=0$, which together with the binding expression in Eq. (1) yields the general results in Eqs. (11) and (12), leads to qualitatively correct predicted behavior for r and, especially, for β'. In this regard, the new assumption is a significant improvement over that employed previously, namely $d\beta'/dm_C=0$ for all m_C. The new auxiliary assumption and the resulting Eqs. (11) and (12) necessarily yield the same r and β' as the previous protocol in the domain of very small m_C, since the two assumptions of the previous protocol are equivalent to our new auxiliary assumption in that same small m_C domain. However, at larger values of m_C, where electrostatic screening of nearest-neighbor charges or groups of charges becomes significant, the predicted values of r and β' of the present approach differ from the predicted values of r and assumed fixed β' of the previous protocol. In particular, both r and β' decline with increasing m_C. In the case of a uniformly charged cylinder with the dimensions and linear charge density of DNA, the present extension of counterion condensation theory predicts r-values that agree well with the results of non-linear Poisson–Boltzmann theory at low-salt concentration, $m_C \leqslant 0.0003$ M, and again at $m_C=0.1$ M, and deviate only modestly $\leqslant 15\%$ at intermediate m_C. Thus, despite its approximate nature, it can provide quantitatively useful estimates of r from low-salt up to 0.15 M, well into the regime of declining r-values. An unexpected bonus is that numerical evaluation of the general results for r and β' in Eq. (11) and Eq. (12) is considerably simpler than solving Manning's Eq. (1) of this paper) for any given value of β'.

Acknowledgments

This work was supported in part by NSF grant MCB-9982735 from the National Science Foundation.

Appendix A: Counterion binding theory for long linear polyions with electrostatically equivalent charges

The polyion possesses N fixed univalent intrinsic charges q that are not necessarily collinear, but which nevertheless occupy equivalent positions in a regular array that is highly extended in one direction. N is so large that end-effects involve only a negligibly small fraction of the intrinsic charges, and the vast majority of the remaining polyion charges are practically equivalent. There is one potential counterion binding site per equivalent charge, but we eliminate from consideration all states that involve local (or global) overcharging. Thus, when the polyion is divided into sections, each with $|z_C|$ consecutive sites, where z_C is the counterion valence, no section ever contains more than a single bound counterion. We consider reactions in which n_C counterions (C) bind to the naked polyion (P) to produce the complex $(D_J(n_C))$, where J denotes the particular configu-

ration of the n_C bound counterions among the N binding sites on the polyion,

$$P + n_C C \rightleftharpoons D_J(n_C) \tag{A1}$$

The concentration of each species (j) is assumed to be sufficiently low that it obeys Henry's Law, and its chemical potential is given by

$$\mu_j = \mu_j^0 + kT\ln X_j \cong \mu_j^0 + kT\ln\left(\frac{m_j}{m_0}\right) \tag{A2}$$

where $m_0 = 55.6$ M is the molarity of the solvent (water), X_j and m_j are the mole fraction and molar concentration, respectively, and μ_j^0 is the standard state chemical potential of the species j. It will be important to note that m_C is the average concentration associated with the chemical potential of the counterion species C, not the local concentration, which may fluctuate about that average. The equilibrium condition for Eq. (A1) is

$$\mu_P + n_C\mu_C = \mu_{D_J(n_C)} \tag{A3}$$

Upon substituting the Eq. (A2) into Eq. (A3) and rearranging there results

$$\frac{m_{D_J(n_C)}}{m_P} = \left(\frac{m_C}{m_0}\right)^{n_C} \exp\left[-(\mu^0_{D_J(n_C)} - \mu_P^0 - n_C\mu_C^0)/kT\right] \tag{A4}$$

We assume that the difference in standard state chemical potentials on the rhs of Eq. (A4) can be partitioned into a contribution due to long-range electrostatic interactions between polyion subunits and a contribution from configurations and interactions within the binding site of a single subunit:

$$\mu^0_{D_J(n_C)} - \mu_P^0 - n_C\mu_C^0 = A_J^{el}(n_C) - A^{el}(0) + n_C\Delta A^{loc} \tag{A5}$$

$A^{el}(0)$ is the sum of all long-range electrostatic interactions between different subunits in the naked polyion P, $A_J^{el}(n_C)$ is the corresponding sum for the complex $D_J(n_C)$, and ΔA^{loc} is the free energy change upon transferring a counterion in its standard state to a single binding 'site' in its standard state. ΔA^{loc} generally contains an electrostatic contribution, as well as contributions from interactions of shorter range and from different configurations of the counterion, polyion, and solvent within the single binding site. The electrostatic part of ΔA^{loc} includes the screened Coulomb interaction between the counterion and binding site (or monomer) charge and also a term that takes into account the activity coefficients of the complex, naked polyion, and counterion. The latter term vanishes when $m_C = 0$ but increases in magnitude with increasing m_C. In any case, ΔA^{loc} is expected to vary with m_C at finite values of m_C. Use of Eq. (A5) in Eq. (A4) gives

$$\frac{m_{D_J(n_C)}}{m_P} = \left(\frac{m_C\beta}{m_0}\right)^{n_C} \times \exp\left[-(A_J^{el}(n_C) - A_J^{el}(0))/kT\right] \tag{A6}$$

where $\beta \equiv \exp[-\Delta A^{loc}/kT]$ is the equilibrium constant for the mole fraction 1.0 standard state. Summing Eq. (A6) over all configurations J for each value of n_C, and then over all possible values of n_C yields

$$\frac{m_D}{m_P} = \sum_{n_C=1}^{N}\left(\frac{m_C\beta}{m_0}\right)^{n_C}\sum_J \exp\left[-(A_J^{el}(n_C) - A^{el}(0))/kT\right] = \chi(m_C, T, N) \tag{A7}$$

where $m_D = \sum_{n_C=1}^{N}\sum_J m_{D_J(n_C)}$ is the total concentration of complexes. The second equality defines the effective grand partition function $\chi(m_C, T, N)$. Combining Eq. (A7) with the conservation relation for the total polyion concentration,

$$m_P^0 = m_D + m_P \tag{A8}$$

yields

$$m_D = \frac{\chi}{1+\chi} m_P^0 \tag{A9}$$

When N is extremely large and the condensed fraction of counterion charge $r \equiv n_C/(N/|z_C|)$ is non-vanishing, there is negligible probability of finding a naked polyion, so $m_D/m_P = \chi(m_C, T, N) \gg 1.0$ and $m_D \cong m_P^0$. In this case (assumed here), the average number of bound counterions per polyion is practically identical to the average number of bound counterions per complex, which is given by

$$\bar{n}_C \equiv \frac{\sum_{n_C=1}^{N} \sum_J n_C m_{D_J(n_C)}}{\sum_{n_C=1}^{N} \sum_J m_{D_J(n_C)}} \equiv m_C \frac{\partial \ln \chi(m_C,T,N)}{\partial m_C} \quad \text{(A10)}$$

wherein the partial derivative on the rhs is taken at constant $A_J^{el}(n_C)$ and β.

We assume that configurations J_u, in which the bound counterions are distributed (nearly) uniformly dominate $\chi(m_C, T, N)$, which is true in fact, though not when the mean-occupation approximation is applied, as noted in the text. Moreover, all sufficiently uniform configurations J_u have practically the same electrostatic free energy, so for those configurations,

$$\exp\left[-(A_{J_u}^{el}(n_C) - A_{J_u}^{el}(0))/kT\right] = \exp\left[-(A^{el}(n_C) - A^{el}(0))\right] \quad \text{(A11)}$$

is independent of the J_u index. Then, $\chi(m_C, T, N)$ becomes

$$\chi(m_C,T,N) = \sum_{n_C=1}^{N} \left(\frac{m_C\beta}{m_0}\right)^{n_C} \exp\left[-(A^{el}(n_C) - A(0))/kT\right] W(n_C) \quad \text{(A12)}$$

where $W(n_C) = \sum_J (1.0)$ is the number of uniform configurations for a polyion with n_C bound counterions. $W(n_C)$ is evaluated as follows. The average number of binding sites per bound counterion is N/n_C. The binding sites on the polyion are divided into n_C contiguous domains each containing N/n_C binding sites. The nearly uniform distributions contain one and only one counterion in every domain. There are N/n_C possible binding sites for each counterion in its domain, so the total number of nearly uniform distributions is approximately

$$W(n_C) = \left(\frac{N}{n_C}\right)^{n_C}. \quad \text{(A13)}$$

Inserting Eq. (A13) into Eq. (A12) yields

$$\chi(m_C,T,N) = \sum_{n_C=1}^{N} \left(\frac{m_C\beta}{m_0}\right)^{n_C} \exp\left[-(A^{el}(n_C) - A^{el}(0))/kT\right] \left(\frac{N}{n_C}\right)^{n_C} \quad \text{(A14)}$$

In principle, ln $\chi(m_C, T, N)$ can be approximated by ln(maxterm), where maxterm denotes the largest term in the sum over n_C. In view of Eq. (A10), it is assumed that this maxterm occurs for $n_C = \bar{n}_C$. The extremum condition for the summand is:

$$0 = \frac{\partial}{\partial \bar{n}_C}\left[\bar{n}_C \ln\left(\frac{m_C\beta}{m_0}\right) - (A^{el}(\bar{n}_C) - A^{el}(0))/kT + \bar{n}_C \ln(N/\bar{n}_C)\right]$$

$$0 = \ln\left(\frac{m_C\beta}{m_0}\right) - \frac{\partial(A^{el}(\bar{n}_C)/kT)}{\partial \bar{n}_C} + \ln(N/\bar{n}_C) - 1 \quad \text{(A15)}$$

After exponentiating Eq. (A15) and multiplying both sides by the fraction of condensed polyion charge $r = \bar{n}_C|z_C|/N$, where $\bar{n}_C$ is the extremum (and average) value, one has

$$r = m_C\left(\frac{\beta}{m_0}e^{-1}\right)|z_C| \exp\left[-\frac{\partial(A^{el}/kT)}{\partial \bar{n}_C}\right] \quad \text{(A16)}$$

Within the counterion condensation model, the polyion charges interact via a screened Coulomb

potential, and the effective value of each polyion charge is $q_{\mathrm{eff}}=(1-r)q$, where q is the electronic charge. For an array of equivalent polyion charges,

$$A^{\mathrm{el}}(\bar{n}_{\mathrm{C}})/kT=(1-r)^2(q^2/\varepsilon kT)N\left(\frac{1}{2}\right)\sum_{l\neq j}\mathrm{e}^{-\lambda r_{jl}/r_{jl}}$$
$$=(1-r)^2L_{\mathrm{B}}NS_j(\lambda) \qquad \text{(A17)}$$

where $L_{\mathrm{B}}\equiv q^2/\varepsilon kT$ is the Bjerrum length, the interaction sum for the jth polyion charge is

$$S_j(\lambda)\equiv\left(\frac{1}{2}\right)\sum_{l\neq j}\mathrm{e}^{-\lambda r_{jl}/r_{jl,}} \qquad \text{(A18)}$$

the Debye screening length is $\lambda=(8\pi(N_{\mathrm{A}}/1000)q^2I/(\varepsilon kT))^{1/2}$, and the ionic strength of the salt is $I=(1/2)m_{\mathrm{C}}(z_{\mathrm{C}}^2+|z_{\mathrm{C}}/z_{\mathrm{d}}|z_{\mathrm{d}}^2)$, where z_{C} is the counterion valence and z_{d} is the coion valence. Use of Eq. (A17), Eq. (A18) and $r=n_{\mathrm{C}}|z_{\mathrm{C}}|/N$ in Eq. (A16) yields

$$r=m_{\mathrm{C}}\beta'|z_{\mathrm{C}}|\mathrm{e}^{-1}\mathrm{e}^{+2(1-r)L_{\mathrm{B}}|z_{\mathrm{C}}|S_j(\lambda)} \qquad \text{(A19)}$$

where $\beta'\equiv\beta/m_0$ is the equilibrium constant for the 1.0 molar standard state. If β' is identified with Manning's free volume, and $S_j(\lambda)$ is evaluated for a line of discrete charges with intrinsic spacing b, which gives $S_j(\lambda)=-(1/b)\ln(1-\mathrm{e}^{-\lambda b})$, then Eq. (A19) becomes identical to Manning's expression in the same limit of univalent polyion charges, and negligible deviation of the small-ion activity coefficients from 1.0. As discussed following Eq. (5) in the text, $\beta'=(1/m_0)\exp[-\Delta A^{\mathrm{loc}}/kT]$ is expected to vary with m_{C} at finite m_{C} in any case.

References

[1] D. Stigter, The charged cylinder with a Gouy double layer, J. Colloid Interface Sci. 53 (1975) 296–306.

[2] D. Stigter, Interactions of highly charged colloidal cylinders with applications to double-stranded DNA, Biopolymers 16 (1981) 1435–1438.

[3] J.J. Delrow, J.A. Gebe, J.M. Schurr, Comparison of hard-cylinder and screened coulomb interactions in the modeling of supercoiled DNAs, Biopolymers 42 (1997) 455–470.

[4] G.S. Manning, The molecular theory of polyelectrolyte solutions with applications to the electrostatic properties of polynucleotides, Q. Rev. Biophys. 11 (1978) 179–246.

[5] G.S. Manning, Limiting laws and counterion condensation in polyelectrolyte solutions. IV. The approach to the limit and the extraordinary stability of the charge fraction, Biophys. Chem. 7 (1977) 95–102.

[6] C.F. Anderson, M.T. Record Jr., Polyelectrolyte theories and their application to DNA, Ann. Rev. Phys. Chem. 33 (1982) 191–222.

[7] G.S. Manning, J. Ray, Counterion condensation revisited, J. Biomol. Struct. Dyn. 16 (1998) 461–476.

[8] J.W. Klein, B.R. Ware, Direct observation of the transition to counterion condensation, J. Chem. Phys. 80 (1984) 1334–1339.

[9] P.J. Heath, J.M. Schurr, Counterion condensation. Effects of site binding, fluctuations in nearest-neighbor interactions, and bending, Macromolecules 25 (1992) 4149–4159.

[10] K.W. Rhee, B.R. Ware, DNA divalent metal cation interactions measured by electrophoretic light scattering, J. Chem. Phys. 78 (1983) 3349–3353.

[11] W.S. Yen, K.W. Rhee, B.R. Ware, Condensation of polyamines onto nucleic acids, J. Phys. Chem. 87 (1983) 2148–2152.

[12] C. Ma, V.A. Bloomfield, Gel electrophoresis measurement of counterion condensation on DNA, Biopolymers 35 (1995) 211–216.

[13] J.M. Schurr, K.S. Schmitz, Dynamic light scattering studies of biopolymers. Effects of charge, shape and flexibility, Ann. Rev. Phys. Chem. 37 (1986) 271–305.

[14] G. Weisbuch, M. Gueron, The surface potential in mixed salt solutions, J. Phys. Chem. 55 (1981) 517–525.

[15] G.V. Ramanathan, Statistical mechanics of electrolytes and polyelectrolytes. 3. The cylindrical Poisson–Boltzmann equation, J. Chem. Phys. 78 (1983) 3223–3232.

[16] M.A. Lampert, The delta-function counterion condensate around a line charge derived from the Fuoss, Katchalsky, and Lifson polyelectrolyte theory, Biopolymers 21 (1982) 159–167.

[17] M. LeBret, B.H. Zimm, Distribution of counterions around a cylindrical polyelectrolyte and Manning condensation theory, Biopolymers 23 (1984) 287–312.

[18] R.W. Wilson, D.C. Rau, V.A. Bloomfield, Comparison of polyelectrolyte theories of the binding of cations to DNA, Biophys. J. 30 (1980) 317–325.

[19] D. Stigter, Evaluation of the counterion condensation theory of polyelectrolytes, Biophy. J. 69 (1995) 380–388.

[20] B.K. Klein, C.F. Anderson, M.T. Record Jr., Comparison of Poisson–Boltzmann and condensation model expressions for the colligative properties of cylindrical polyions, Biopolymers 20 (1981) 2263–2280.

[21] B.-Y. Ha, A.J. Liu, Counterion mediated attractions between two like-charge rods, Phys. Rev. Lett. 79 (1997) 1289–1292.

[22] B.-Y. Ha, A.J. Liu, Effect of non-pairwise-additive interactions on bundles of rodlike polyelectrolytes, Phys. Rev. Lett. 81 (1998) 1011–1014.
[23] V.A. Bloomfield, DNA condensation by multivalent cations, Biopolymers 44 (1997) 269–282.
[24] J.X. Tang, P.A. Janmey, The polyelectrolyte nature of F-actin and the mechanism of actin bundle formation, J. Biol. Chem. 271 (1996) 8556–8563.
[25] J.X. Tang, T. Ito, T. Tao, P. Traub, P.A. Janmey, Opposite effects of electrostatics and steric exclusion on bundle formation by F-actin and other filamentous polyelectrolytes, Biochemistry 36 (1997) 12600–12607.
[26] M.O. Fenley, G.S. Manning, W.K. Olson, Approach to the limit of counterion condensation, Biopolymers 30 (1990) 1191–1203.
[27] M.O. Fenley, G.S. Manning, N.L. Marky, W.K. Olson, Excess counterion binding and ionic stability of kinked and branched DNA, Biophys. Chem. 74 (1998) 135–152.
[28] R.M. Nyquist, B.-Y. Ha, A.J. Liu, Counterion condensation in solutions of rigid polyelectrolytes, Macromolecules 32 (1999) 3481–3487.
[29] G.S. Manning, Counterion condensation theory constructed from different models, Physica A 247 (1996) 236–253.
[30] G.S. Manning, Counterion condensation on a helical charge lattice, Macromolecules 34 (1999) 4650–4655.
[31] H. Qian, J.A. Schellman, Transformed Poisson–Boltzmann relations and ionic distributions, J. Phys. Chem. B 104 (2000) 11528–11540.
[32] M. Deserno, C. Holm, S. May, Fraction of condensed counterions around a charged rod: comparison of Poisson–Boltzmann theory and computer simulations, Macromolecules 33 (2000) 199–206.
[33] M.C. Olmsted, C.F. Anderson, T.M. Record Jr., Monte Carlo description of oligoelectrolyte properties of DNA oligomers: range of the end effect and the approach of molecular and thermodynamic properties to the polyelectrolyte limits, Proc. Natl. Acad. Sci. USA 86 (1989) 7766–7770.
[34] M.C. Olmsted, C.F. Anderson, M.T. Record Jr., Importance of oligoelectrolyte end effects for the thermodynamics of conformational transitions of nucleic acid oligomers: a grand canonical Monte Carlo analysis, Biopolymers 31 (1991) 1593–1604.
[35] V.M. Stein, J.P. Bond, M.W. Capp, C.F. Anderson, M.T. Record Jr., Importance of coulombic end effects on cation accumulation near oligoelectrolyte B-DNA: a demonstration using 23 Na NMR, Biophys. J. 68 (1995) 1063–1072.
[36] W. Zhang, J.P. Bond, C.F. Anderson, T.M. Lohman, M.T. Record Jr., Large electrostatic differences in the binding thermodynamics of a cationic peptide to oligomeric and polymeric DNA, Proc. Natl. Acad. Sci. USA 93 (1996) 2511–2516.
[37] M.T. Record Jr., W. Zhang, C.F. Anderson, Analysis of effects of salts and uncharged solutes on protein and nucleic acid equilibria and processes: a practical guide to recognizing and interpreting polyelectrolyte effects, Hofmeister effects, and osmotic effects of salts, Adv. Prot. Chem. 51 (1998) 281–353.
[38] W. Zhang, H. Ni, M.W. Capp, C.F. Anderson, T.M. Lohman, M.T. Record Jr., The importance of coulombic end effects: experimental characterization of the effects of oligonucleotide flanking charges on the strength and salt dependence of oligocation (L8+) binding to single-stranded DNA oligomers, Biophys. J. 76 (1999) 1008–1017.
[39] E. Raspaud, M. da Conceicao, F. Livolant, Do free counterions control the osmotic pressure?, Phys. Rev. Lett. 84 (2000) 2533–2536.
[40] P.L. Hansen, R. Podgornik, A.V. Parsegian, Osmotic properties of DNA: critical evaluation of counterion condensation theory, Phys. Rev. E 64 (2001) 64–68.
[41] S. Sugai, K. Nitta, Surface electric potential of a rodlike polyelectrolyte, Biopolymers 12 (1973) 1363–1376.